PRACE NAUKOWE Wyższej Szkoły Pedagogicznej w Częstochowie
Seria: FIZYKA 1999, z. II

M. MAKOWSKA-JANUSIK[a] , I.V. KITYK, J. BERDOWSKI

Institute of Physics WSP, Czestochowa, Poland
[a] Scholarship-holder of Foundation for Polish Science '99

A. MEFLEH

IMP-CNRS-GP2M, Universite de Perpignan, 52, Avenue de Villeneuve, 66860 Perpignan, France
E-mail:mefleh@univ-perp.fr

Acoustically Induced Nonlinear Optics in $Ca_4GdO(BO_3)_3$ Nanocrystallites Embedded within the Olygoether Matrices

ABSTRACT: Acoustically induced optical phenomena in GdCOB ($Ca_4GdO(BO_3)_3$ nanocrystallites embedded within the olygoether photopolymer matrices have been studied using experimental nonlinear optics methods. Acoustically induced two-photon absorption (TPA) and second harmonic generation (SHG) for the pumping wavelength of the YAG:Nd laser (λ = 1.06 mm) have been measured. We have found that with an increasing acoustical wave power, the SHG for YAG:Nd laser (λ = 1.06 mm) for the double frequency (λ = 0.53 mm) increases and achieves its maximum value at acoustical intensity about 1.75 W/cm^2 and acoustical frequency about 12 kHz. The absolute SHG values were more than 45 % less comparing with d_{222} tensor of the KDP single crystals for the λ = 1.06 mm. With decreasing temperature, the acoustically induced SHG signal strongly increases below 16 K. A correlation between the photoinduced nonlinear optical response and low-frequency Raman intensities have been found. The maximal acoustically induced SHG have been observed at nanocrystallite concentrations about 2.1 % (in weighting units) and at acoustical power about 5.8 W/cm^2 for the nanocrystallite sizes within the range 50...60 nm. The observed dependencies possess essentially nonlinear features This one reflects nonlinear superposition of the nonlinear optical susceptibilities within the particular nanocrystallites electropoled in external electric field. At the same time we have observed giant increase of the TPA (for the W = 1.8 W/cm^2) at high hydrostatic pressures (about 16 GPa) and low temperatures (below 16 K). This one reflects complicated influence of the electron-phonon interactions on the observed dependencies. The corresponding evaluations are presented with using *ab initio* band energy calculations and taking into account of anharmonic electron-phonon interactions.

1. Introduction

One can recently observe an increasing interest in several nonlinear-optical borate such as b-BaB_2O_4 (BBO) and LiB_3O_5 (LBO) [1, 2]. In work [3] linear- and nonlinear-optical properties of new synthesized ($Ca_4GdO(BO_3)_3$) single crystals were discovered. These single crystals are absolutely insensitive to moisture. The specimens are transparent in visible and in the near IR spectral range (from 0.32 to 2.7 mm). The

value of damage threshold is of about 1.9 GW/cm^2 and the efficiency of the optical second harmonic generation (SHG) is higher than 50 % for the 1.06 mm YAG:Nd laser wavelength. Coming out from a similarity of the mentioned crystals to the other crystals, for example to $Li_2B_4O_7$ (TBL) single crystals one can predict that the mentioned crystals should possess also the good acoustical properties. Moreover presence of the heavy Gd ions could stimulate different kinds of the acoustically-induced phenomena. On the other side the GdCOB promise also to be a good NLO chromophores for possibility of embedding in the different polymer matrices first of all due to the good solution features. As a consequence in the present work experimental investigations of acoustically induced nonlinear optical properties of GdCOB nanocrystallites embedded within the photopolymer matrices will be presented.

In the Sec. 2 the experimental data concerning specimen preparation and their measurements are presented. Sec. 3 is devoted to the obtained results and to the explanation of the observed phenomena.

2. Experimental details

2.1. Sample preparation

GdCOB single crystal is one of the calcium-rare-earth oxoborate single crystals with a general chemical contents of $Ca_4GdO(BO_3)_3$. These single crystals are grown in the monoclinic biaxial crystal system. The unit cell parameters are as follow: a = 0.8095(7) nm, b = 1.60186(6) nm and c = 0.3558(8) nm, and angle b = 101.26° [3]. The crystals belong to C_m space group and number of unit formula is Z = 2. Two types of Ca^{2+} ions occupy distorted octahedral sites. BO_3 triangles form three-dimensional network. At the same time two kinds of boron sites, B(1) and B(2) posses threefold coordination.

The investigated single crystals were grown using the well known Czochralski method starting from the solid state reactions between the Gd_2O_3, $CaCO_3$ and H_3BO_3 or B_2O_3 which were taken in a stoichiometry proportion. The single crystals have parallelepiped form of typically 5 x 5 x 10 mm dimensions. The mixture was heated at 1230 K during 18 h, cooled and ground, and then heated again at 1625 K for 22 h. Control of the phase single crystalline homogeneity have been carried out using DRON 5.0 X-ray diffractometer. After the single crystals have been crushed and melt both mechanically as well as by ultrasound methods in order to obtain the nanopowder nanocrystallites.

The synthesized nanocrystalline samples had powder-like form with diameter sizes lying within the 30 – 70 nm. The powder-like specimens were dissolved in the liquid oligoetheracrylate photopolymer matrices (more details see in the Ref. [4]) The solidification process and electropoling homogenization have been carried out using a method described in the Ref. [4]. Nitrogen laser (λ = 337 nm) with the light power about 35 W/cm^2 was used for the solidification.

Afterwards the $LiNBO_3$ (LNB) piezoelectric electrodes have been attached to the mentioned materials using CYATYM glue. The equipment allows us continuously to

vary specimen thickness within the 0.3 ... 0.9 cm with the step of the 0.1 mm. Homogenization of the mixture have been carried out using ultrasound mixing and crushing and control of the specimen homogeneity have been carried out using the optical polarized method. We have revealed that the deviation from the homogeneity was less than 4.6 % through the specimen surface.

2.2. Measurement setup

The excitation was provided by picosecond light pulses of λ = 1.06 mm of YAG:Nd laser. The acoustical signal power has been applied to the LNB specimens by piezo-electric transducers in the c_{66} prolonged tensor geometry with the varied acoustical frequencies (80 Hz ... 1.2 MHz). The laser light was polarized using a rotating Fresnel polarizer and the output light intensities were detected using a FEU-79 (FEU-39) photomultipliers. The measurements were carried out in the single-pulse regime, with a pulse frequency repetition of 12 Hz and the tunable pulse duration within the 0.6 ... 50 ps. Such short-time kinetics allows us to avoid the specimen heating. The pumping laser beams have been scanned through the specimen surface in order to avoid the specimen nonhomogenuity contributions. The measurements have been carried out both for the transmitted beam and for the reflected light beam case. Therefore for every thickness we have obtained more than 120 measured points for the transmitted T, reflected R and scattered R_s light intensities. Precision of the T and R evaluations was best than 5 %.

The laser beam has been diafragmed to obtain the light profile inhomogeneouity (usually of the gaussian form) not less than 92 % of the maximum light intensity for the energy powers lying within the 0.75 ... 1.1 GW/cm^2. Measurements devices both for the transparent and reflected channel have been synchronized. Absorption coefficient was calculated by expression:

$$K(I) = 1/dln\,[(1 - R(I))/2T(I) + ((1 - R(I))^2/4R(I)^2)], \qquad (1)$$

Evaluating the dependence of the K versus the I the TPA coefficient b has been extracted. Statistical treatment using the χ^2 Student approach gives a reliability of the obtained data not worse than 0.03. Independent measurements of the TPA for the proper oligoether matrices have been done. These were necessary to eliminate the influence of photopolymer matrix background. The TPA signal was extracted from the intensity-dependent transparency T measurements. Simultaneously we extracted influence of linear absorption (220 cm^{-1}, λ = 530 nm) and of Fresnel reflection 0.051. The choice of the oligoetheracrylate matrices is caused by the relatively low value of their TPA coefficient (below 0.002 cm/GW) and close values of the corresponding refractive indices (see for example Ref. 5). The averaging statistics over the sample surface was performed to avoid a space nonuniformity in the sample distribution within the photopolymer oligoetheracrylate matrices.

To exclude an influence of the hyper-Raman scattering, we have carried out additional investigations of the scattered light up to 2600 cm^{-1}, starting from the wavelength λ = 441 nm have been done. Hyper-Raman maxima within the 1200 cm^{-1} ... 1800 cm^{-1} spectral range with intensities at least 9 times weaker than the transmitted

light intensity. In the case of the Raman and hyper-Raman measurements we have used argon laser at 441 nm Ar^+ laser line and SPM-3 spectrometer. A position-sensitive photomultiplier calibrated using helium-neon gaseous mixture discharge was used to detect the integrated scattering background .

For optical measurements under applied hydrostatic pressures we have constructed a special thermo-baro chamber with saphire windows that allowed to perform the corresponding measurements in the high-pressure atmosphere within the temperature range 4.2 – 300 K. For temperatures below 77 K a special type of diamond anvil have been used.

The pressure and the temperature were varied within the 0.1 – 20 GPa and 4.2 – 300 K regions, respectively. Precision of the pressure and temperature stabilization was equal to ± 0.32 GPa and to ± 0.12 K, respectively. All the measured optical parameters were averaged over a great number of pulses (about 160 – 180) for every p-T point. Afterwards, we have performed a fitting procedure using a spline smoothing and Student statistical procedure with parameter χ^2 not worse than 0.02.

We used a mixture of 12:3:3 of buthanol:ethanol:liquid nitrogen or liquid argon as the pressure medium. Ruby laser fluorescence was used for hydrostatic-pressure determination of pressure gradients. The setup allows us to carry out the TPA measurement in the transparent geometry (parallel spreading of the pumping and probing beams). The intensity of the laser beams was varied using neutral density filters. A time-delay between the pump and tunable probe pulse was obtained using the $Li_2B_4O_7$ single crystal.

3. Experimental results and discussion

In the Fig. 1 we present measured pressure-temperature (p-T) dependencies of the TPA for the GdCOB nanocrystallites embedded within the electropoled photopolymer matrices. After the varying of the nanocrystallite sizes and concentrations of the nanoparticles we have found that the maximal TPA coefficients are achieved for the acoustical power about 1.8 W/cm^2 and acoustical wave frequencies about the 80 ... 82 kHz. Essential increase of the acoustically induced TPA signals have been observed at the nanocrystallite sizes within the range 50 ... 60 nm. Optimal concentration of the nanocrystallites lies within 2 ... 5 % (in weighting ratio).

The measured acoustically induced dependencies of the TPA (d_{2222} tensor geometry) for the optimal nanocrystallite sizes (50 ... 60 mm) and concentration (about 3.8 %) versus temperature T and hydrostatic pressure p show that decreasing temperature leads to a decrease of the TPA within the pressure range 7 ... 12 GPa. Simultaneously within the pressure range 15 ... 21 GPa we observed drastical increase of the TPA coefficients d_{1111} at least five times.

Another interesting effect have been observed for SHG stimulated by the acoustical wave. The used nanocrystallite parameters have been similar to the described for the TPA. But for convenience we will present only dependencies of the SHG versus nanocrystallite sizes and acoustical power (see Fig. 2). One can see essentially nonlinear dependence of the acoustically-induced SHG (AISHG) versus nanocrystallite concentration and acoustical power. For the low acoustical powers below 3.8 W/cm^2

and low concentrations of the nanocrystallites (0.6 ... 4.3 %) one can see quasi-linear increase of the output SHG (in the d_{111} tensor geometry) with the increase of the above mentioned parameters. With the next increase of the above mentioned parameters the AISHG signals are saturated and at acoustical power higher than 5.8 W/cm^2 the output SHG signal becomes to decrease up to the 8.2 W/cm^2. With the following increase of the acoustical powers the output AISHG begins once more to increase. At concentrations of the nanocrystallits higher than 7.8 % acoustically-induced dependencies become more smooth.

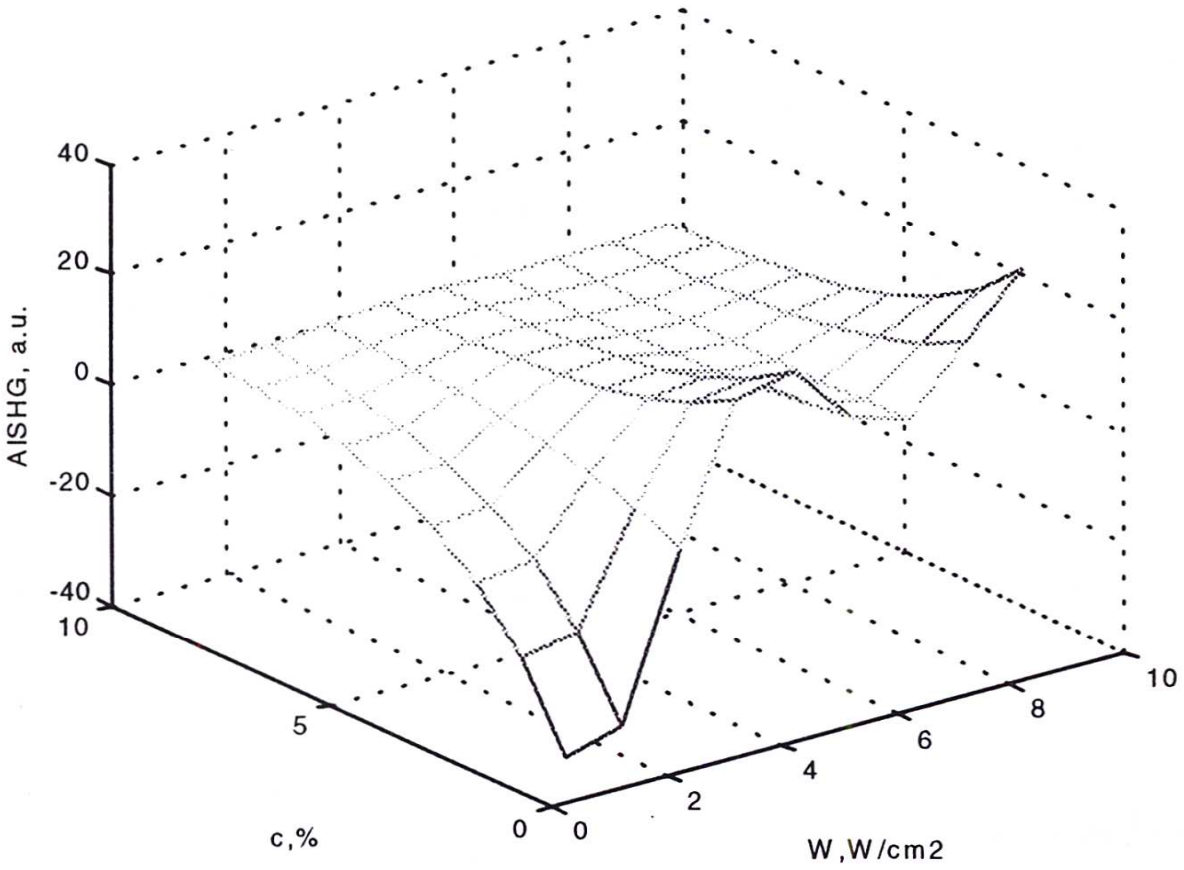

Fig. 1. Dependence of the TPA versus temperature T and pressure p.

Simultaneously the observed p-T dependences are similar to the observed ones for the modified fullerenes [10]. The main difference with the mentioned case consists in the size-dependent confined effects for the mentioned nanocrystallites.

One can assume that the observed modulated-like structure could be caused by anharmonic electron-quasi-phonon interactions within and outside the particular nanocrystallites. Pressure and temperature continuously vary the corresponding interaction parameters. These external susceptibilities have different sign of contributions to the final output susceptibilities and as a consequence during the variations of the p - T we have a competition of these factors. A similar effect is caused by concentration-dependent changes and distances between the particular nanocrystallites.

The discovered dependencies could be used as sensitive tools for the p-T detection with the simultaneous control of the acoustical wave intensity.

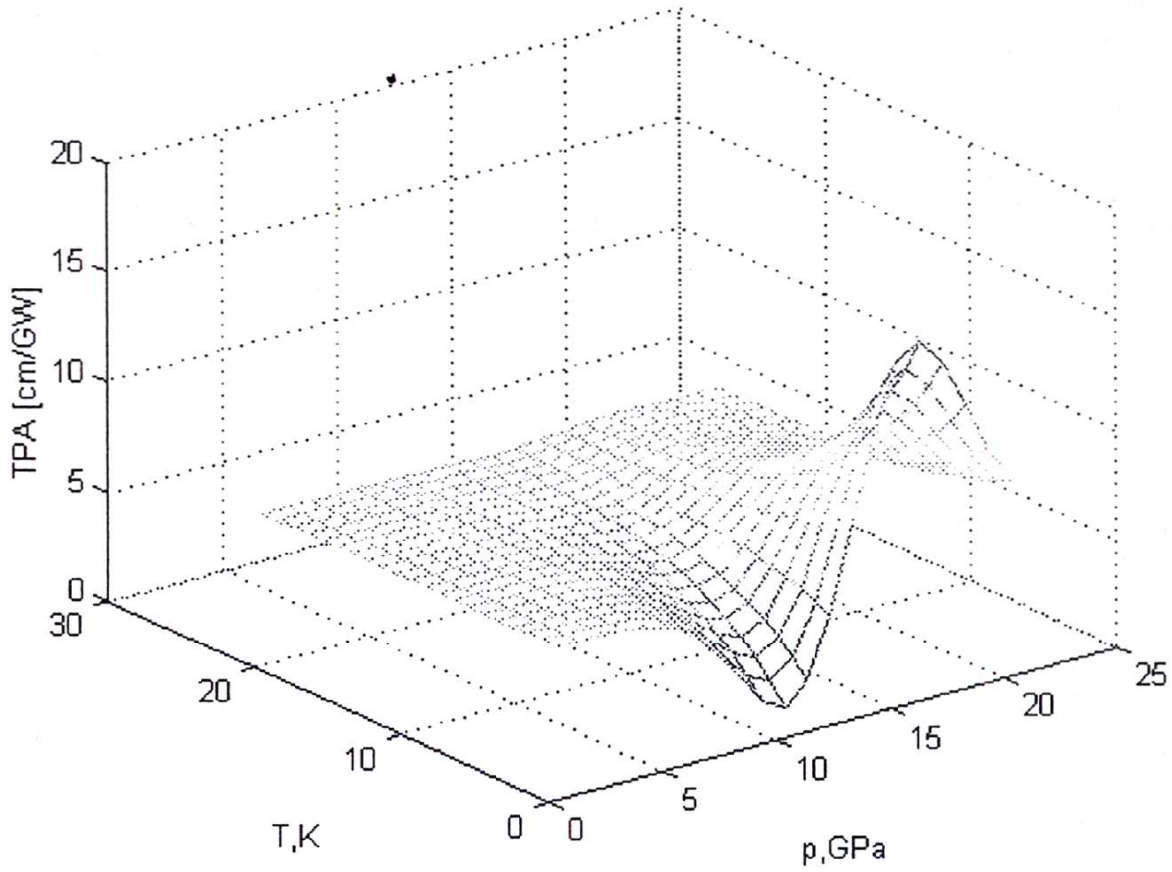

Fig. 2. Dependence of the acoustically-induced SHG versus nanocrystallite concentrations c and acoustical power W at 4.2 K.

Conclusions

We have revealed that the maximal TPA coefficients are achieved for the acoustical power about 1.8 W/cm^2 and acoustical wave frequencie within 80 … 82 kHz. Essential increase of the acoustically induced TPA signals have been observed at the nanocrystallite sizes lying within the range 50 … 60 mm. Optimal concentration of the nanocrystallites lies within range 2…5 % (n at. Weight.units).

Nonlinear dependence of the AISHG versus nanocrystallite concentration and acoustical power observe quasi-linear increase of the output SHG (in the d_{111} tensor geometry) have been observed for the low acoustical power below 3.8 W/cm^2 and low concentrations (0.6…4.3 %) one can. With the next increase of the above mentioned parameters the AISHG signals was saturated and at acoustical power higher than 5.8 W/cm^2 the output SHG signal becomes to decrease up to the 8.2 W/cm^2. With the following increase of the acoustical power the output AISHG begins once more to increase. At concentrations of the crystallites higher than 7.8 % acoustically-induced dependencies become more smooth that reflects increasing role of the internano-crystallite interactions.

References

1. C. Chen, B. Wu, A. Jiang and G. You, **Sci.Sin**, **B28**, 235-243, (1985).
2. C. Chen, Y. Wu, A. Jiang, B. Wu, G. You, R. Li, and S. Lin, , *JOSA*, **B6**, 616-621, (1989).
3. G. Aka, A. Kahn-Harari, E. Mougel, D. Vivien, E. Salin, P. Coquelin, P. Colin, D. Pelenc, and J.P. Damelt, *JOSA*, **B14**, 2238-2247, (1997).
4. I.V. Kityk, R.I. Merwinskii, J. Kasperczyk, S. Jossi, *Materials Letters*, 1996, V. 27, 233.
5. J. Wasylak, J. Kucharski, I.V. Kityk, B. Sahraoui, *J.Appl.Phys.*, 1999, V. 85, 425.
6. I.V. Kityk, A. Mefleh, *Physica B: Condensed Matter*, 1999, V.262, 170.
7. M. Czerwinski, J. Bielieninik, J. Napieralski, I.V. Kityk, J. Kasperczyk, R.I. Merwinskii. *Europ.Polym.Journ.*, 1997, V.33, 1441 – 1447.
8. B. Sahraoui, I.V. Kityk, M. Czerwinski, J. Kasperczyk, *High Performance Polymers*, 1997, V. 9, pp. 51 – 60.
9. M. Czerwinski, R.I. Merwinskii, M. Kulesza, I.V. Kityk, J. Kasperczyk, *Mater.Chem. and Physics*, 1998, V. 56, 713.
10. B. Sahraoui, I.V. Kityk, X. Nguyen Phu, P. Hudhomme, A. Gorgues, *Phys.Rev.*, 1999, V. B 59, N 13.
11. O.I. Shpotyuk, J. Kasperczyk, I.V. Kityk, *J.Non-Crystal.Solids*, 1997, V.215, 218.
12. I.V. Kityk, E. Jakubczyk, Z. Mandecki, *Mater.Sci.&Engin.*, 1997, V. A226, 1045.